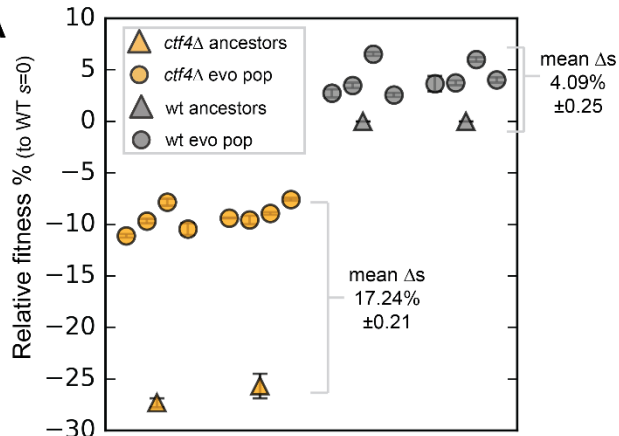


# 1 Supplementary figures

2 **Figure S1. Related to Fig. 1. A**  
 3 (A) Fitness of the *ctf4Δ*  
 4 (yellow) and wt (grey)  
 5 ancestors and of 16 evolved  
 6 populations derived from them  
 7 (8 each), relative to wt cells  
 8 (*s*=0). Error bars represent  
 9 standard deviations. Note that  
 10 this panel shows the fitnesses  
 11 of populations, whereas Fig.  
 12 1C shows the fitness of clones  
 13 isolated from populations. (B)  
 14 Bulk segregant analysis of  
 15 evolved clones: One clone per  
 16 population was crossed with a  
 17 wt ancestor and subjected to  
 18 bulk segregant analysis. For  
 19 each clone, the mutations  
 20 found to strongly segregate  
 21 (>70%) with the evolved  
 22 phenotype are reported. (C)  
 23 Extract from Table S2: GO  
 24 term that are enriched in the  
 25 genes that were found to be  
 26 either strongly significantly  
 27 selected or segregating with  
 28 the evolved phenotype by bulk  
 29 segregant analysis.



30  
31  
32  
33  
34

**B**

Clone	Gene	Nucleotide change	AA and regulatory change	Segregation
EVO1-7	<i>IXR1</i>	1393 A→C	T465P	97%
	<i>RAD9</i>	3286 G→A	G1096E	74%
	<i>TIR1</i>	426-464del	139-188del	91%
EVO2-10	<i>PSF3</i>	134 G→A	S45N	88%
	<i>NVJ2</i>	-559 G→C	promoter	84%
EVO3-12	<i>SIR4</i>	1877 C→A	S626*	97%
	<i>IXR1</i>	922 C→T	Q308*	94%
	<i>MMS1</i>	2170 G→T	A724S	88%
	<i>DPB11</i>	1804 +A	S608*	76%
EVO4-2	<i>RPS28B</i>	42 -G	terminator	90%
	<i>IXR1</i>	79 C→T	Q27*	80%
	<i>SIR4</i>	3140 C→T	S1047F	95%
EVO5-11	<i>RAD9</i>	2628 +A	K883*	81%
	<i>RPS28B</i>	42 -G	terminator	76%
	<i>CDD1</i>	68 +TTTT	terminator	73%
	<i>SLD5</i>	388 G→A	E130K	83%
EVO6-1	<i>CTH1</i>	4 A→G	M2V	71%
	<i>GIR2</i>	-197 T→C	promoter	71%
	<i>IXR1</i>	1263 C→G	Y421*	94%
EVO7-7	<i>SIR3</i>	32 G→A	W11*	79%
	<i>SMC2</i>	940 C→A	R164S	71%
	<i>UTR2</i>	-524 C→T	promoter	80%
	<i>PSF3</i>	53 G→T	C18F	93%
EVO8-9	<i>CTR9</i>	976 T→A	L326I	84%
	<i>DSF2</i>	772 +A	T263*	84%
EVO8-9	<i>PSF1</i>	599 T→A	I200N	82%

35  
36

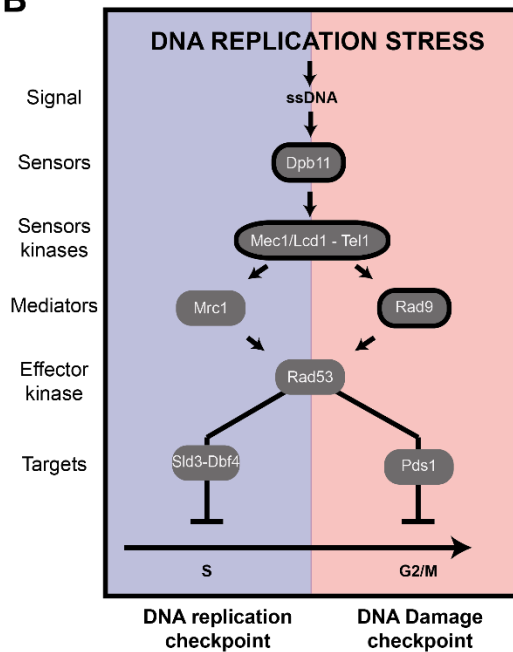
**C**

#Term ID	Term description	Observed gene count	Background gene count	False discovery rate
GO:0006259	DNA metabolic process	13	499	0.00011
GO:0006261	DNA-dependent DNA replication	7	117	0.00011
GO:0006281	DNA repair	11	296	0.00011
GO:0006302	double-strand break repair	7	131	0.00013
GO:0051276	chromosome organization	11	566	0.0011
GO:0007049	cell cycle	12	716	0.0019
GO:0071103	DNA conformation change	5	117	0.0039
GO:0006343	establishment of chromatin silencing	2	4	0.0041
GO:0006310	DNA recombination	6	227	0.0073
GO:0007076	mitotic chromosome condensation	2	11	0.0128
GO:0006323	DNA packaging	3	56	0.02
GO:0044773	mitotic DNA damage checkpoint	2	17	0.025
GO:1903047	mitotic cell cycle process	6	310	0.0272

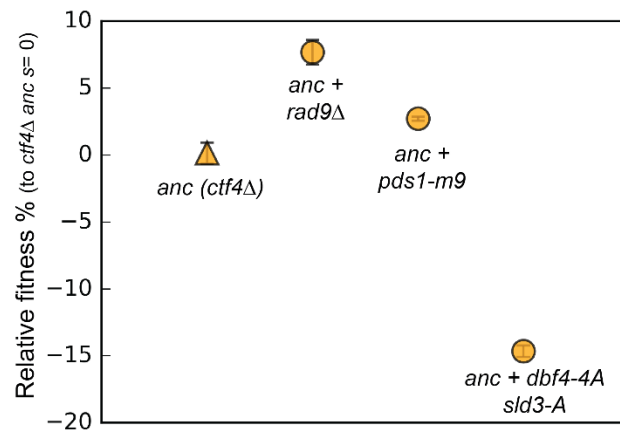
**A**

Gene	Unique hits	Nucleotide change	AA change	Type	Note
<i>RAD9</i>	5	2628 +A	frameshift	indel	K883*
<i>RAD9</i>	1	3017 T→G	L1006W	substitution	
<i>RAD9</i>	1	1904 +A	frameshift	indel	D638*
<i>RAD9</i>	1	3287 G→A	G1096E	substitution	
<i>RAD9</i>	1	3835 G→A	E1278K	substitution	
<i>MEC1</i>	1	3917 C→T	A1306V	substitution	
<i>TEL1</i>	1	2282 C→A	T2028K	substitution	kinase domain
<i>LCD1</i>	1	536 G→A	R179H	substitution	
<i>DPB11</i>	1	1804 +A	frameshift	indel	S608*

**B**



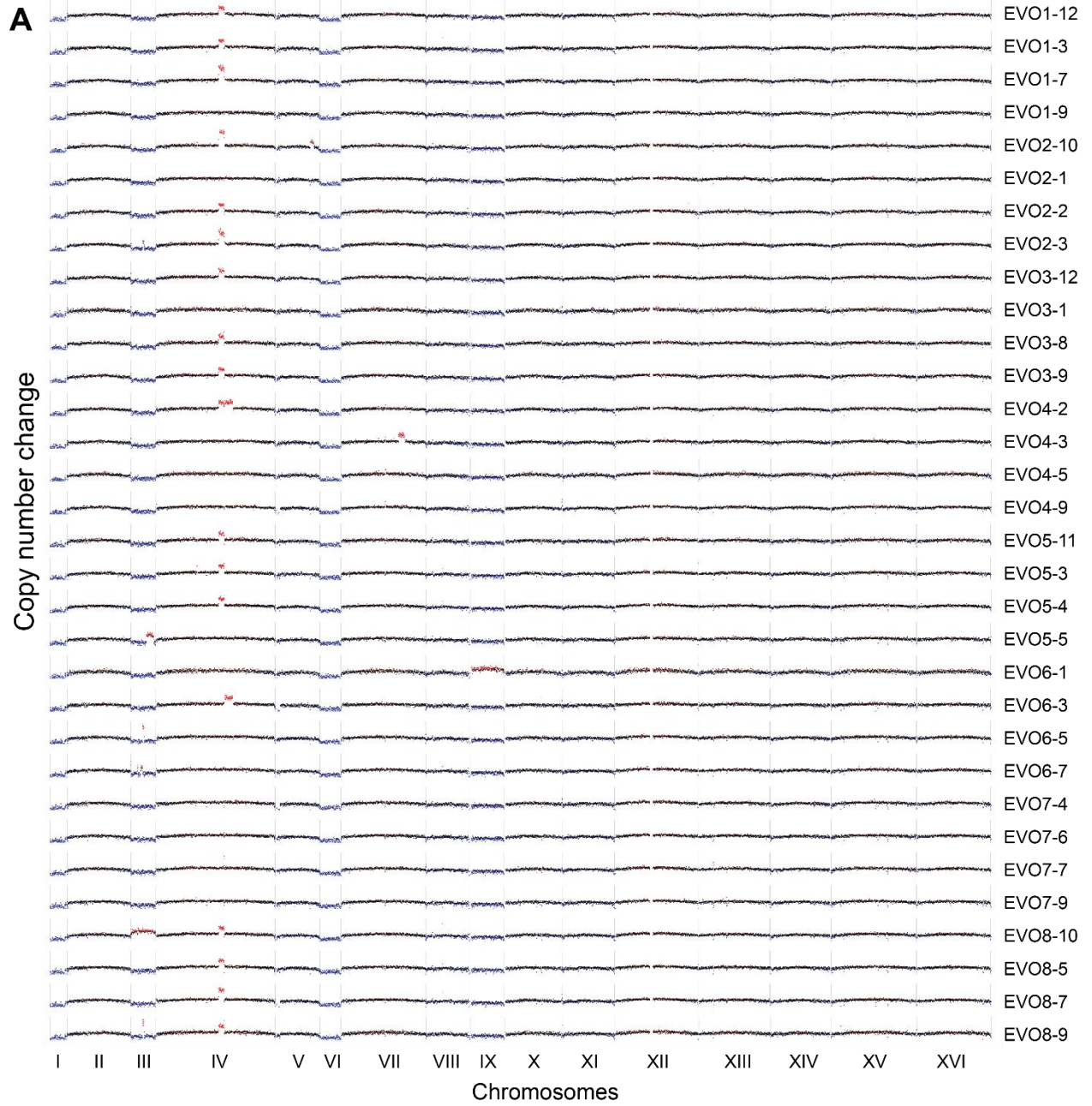
**C**



37

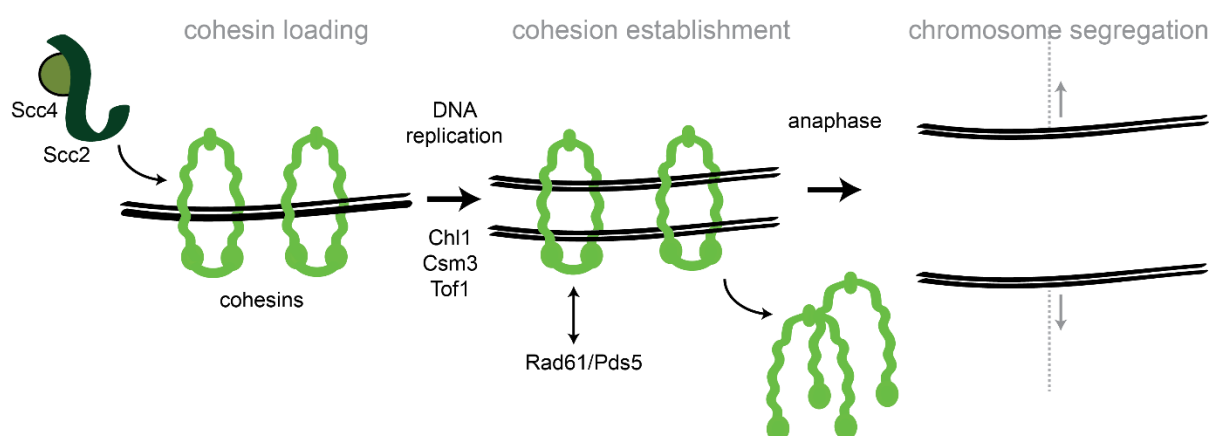
38 **Figure S2. Related to Fig. 2 (A)** Mutations affecting components of the DNA damage checkpoint that were  
 39 found in evolved clones. **(B)** Schematic representation of the checkpoint signaling cascade induced by DNA  
 40 replication stress. In blue (left) the DNA replication checkpoint, which delays S phase by phosphorylating  
 41 Sld3 and Dbf4. In red (right) the DNA damage checkpoint, which induces a mitotic delay by phosphorylating  
 42 Pds1. Factors highlighted in bold were found mutated in evolved lines. Some of the checkpoint factors (in  
 43 the middle of the panel) play a role in both checkpoint responses, although this double role is likely not  
 44 exerted simultaneously and may depend on the dynamics of the upstream checkpoint reactions. **(C)** The  
 45 fitness of ancestral *ctf4Δ* strains carrying mutations affecting the DNA replication checkpoint signaling  
 46 cascade at different levels, relative to the *ctf4Δ* ancestor ( $s=0$ ). Error bars represent standard deviations.

47



**B**

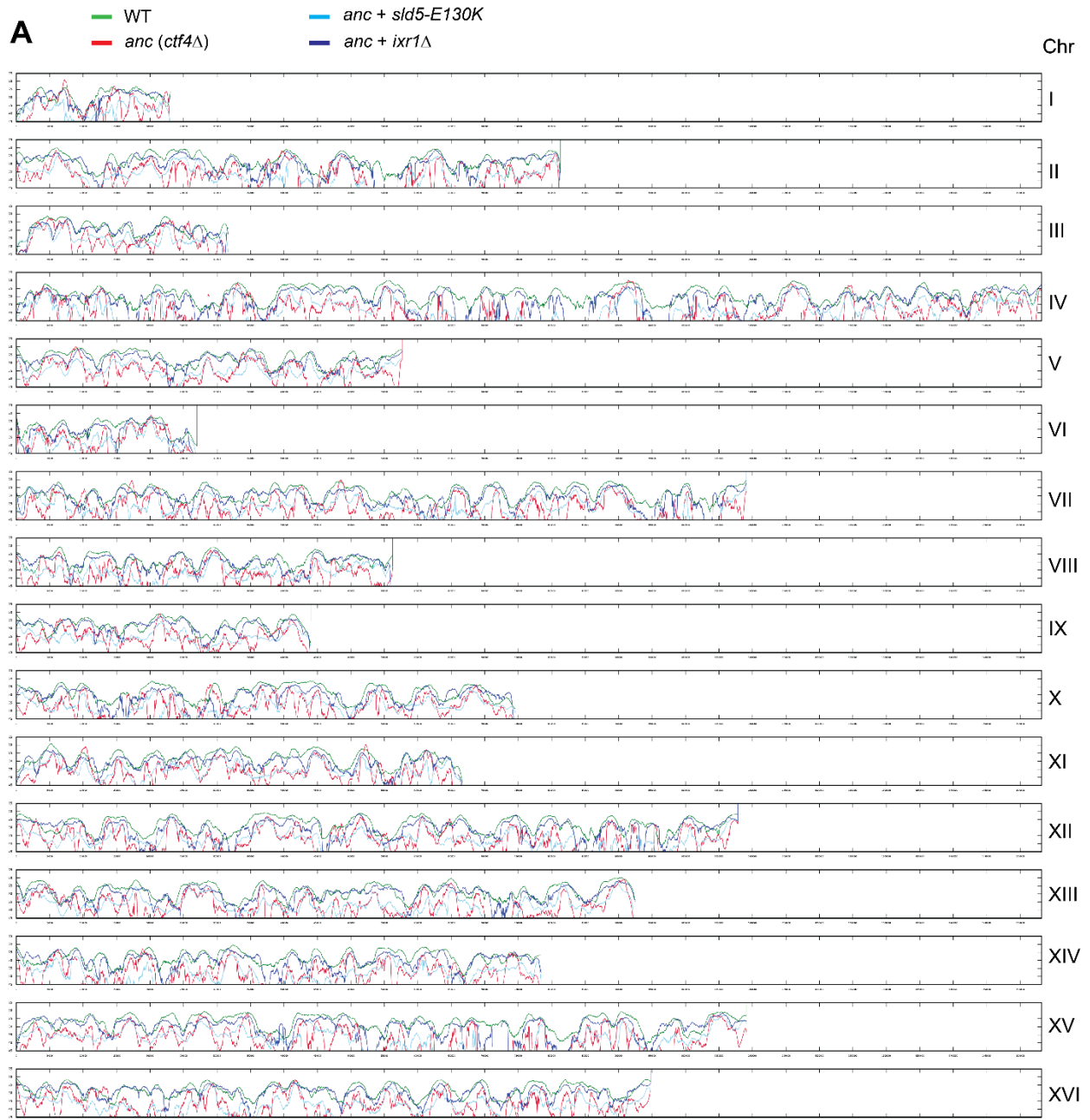
Gene	Unique hits	Nucleotide change	AA change	Type	Note
<i>RAD61</i>	1	2628 T→A	Promoter	substitution	
<i>CHL1</i>	1	2050 G→A	D684N	substitution	helicase domain
<i>PDS5</i>	1	204 A→C	K68N	substitution	
<i>SMC2</i>	1	940 C→A	R314S	substitution	
<i>TOF1</i>	1	1244 C→A	P415Q	substitution	
<i>CSM3</i>	1	370 G→C	V124L	substitution	

**C**

49

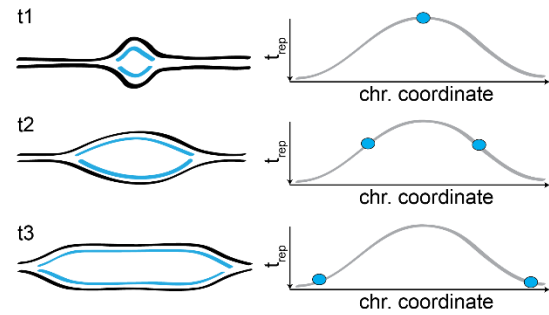
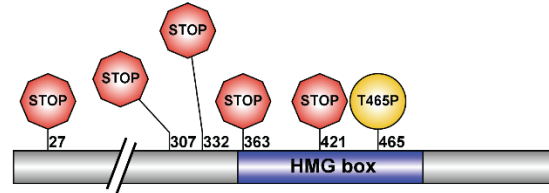
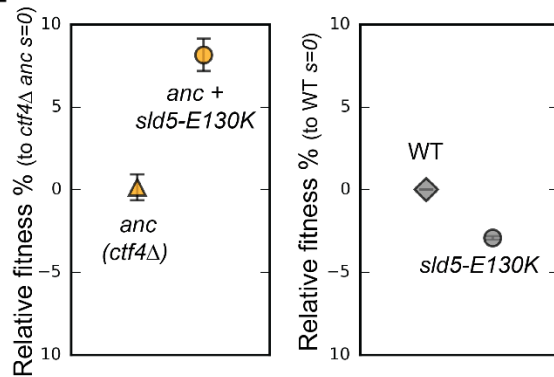
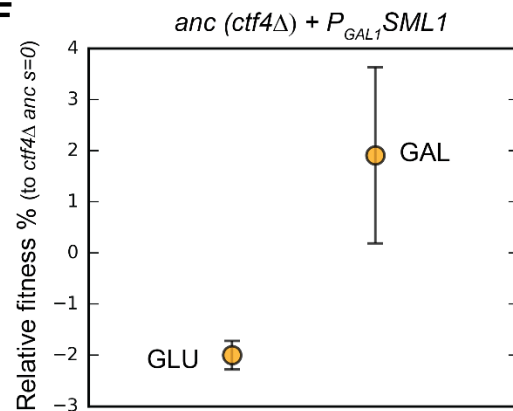
50 **Figure S3. Related to Fig. 3. (A)** CNVs affecting the genome of the 32 isolated evolved clones. Red  
 51 highlights gains, blue highlights losses. Note that the aneuploidies affecting chromosome I, III, VI and IX,  
 52 all of which are small chromosomes, may be due to the altered ancestral karyotype. We retrospectively  
 53 found that ancestral *ctf4Δ* clones carried extra copies of these chromosomes, likely caused by chromosome  
 54 mis-segregation acquired during strain construction or the initial pre-culture. Many evolved clones lose one  
 55 of the two copies of these chromosomes during evolution arguing that aneuploidy for these chromosomes  
 56 does not confer a long-term fitness advantage. **(B)** Mutations affecting genes implicated in chromosome  
 57 segregation that were found in evolved clones. **(C)** Schematic representation of cohesion establishment:  
 58 the cohesin loading complex (Scc2-Scc4) loads the cohesin ring onto chromosome in G1. With the passage  
 59 of the replisomes during DNA replication, cohesion between sister chromatids is established. At the onset  
 60 of anaphase, cohesin is cleaved to allow cells entering anaphase and segregating the chromosomes.  
 61 Proteins whose genes were mutated in evolved strains are indicated next to the steps where they are  
 62 believed to act.

63



**B**

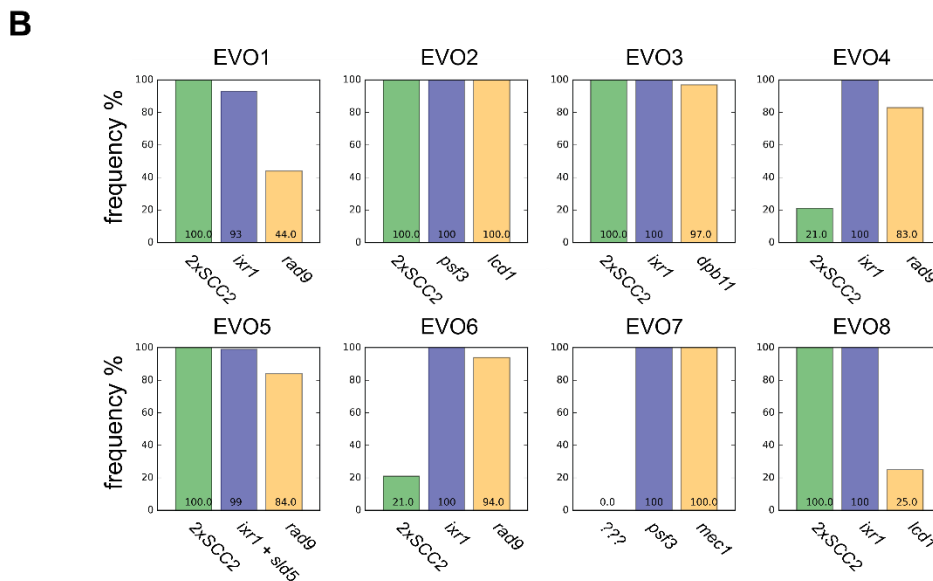
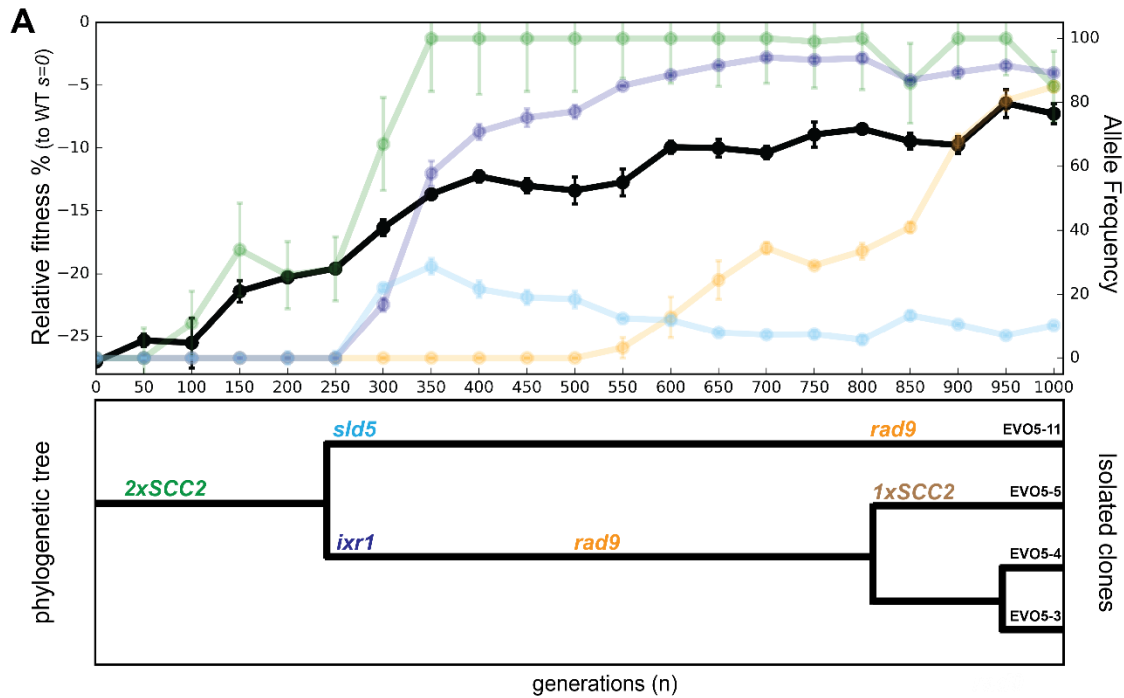
Gene	Unique hits	Nucleotide change	AA change	Type	Note
<i>IXR1</i>	1	1393 A→C	T465P	substitution	HMG domain
<i>IXR1</i>	1	922 C→T	Q307*	substitution	
<i>IXR1</i>	1	79 C→T	Q27*	substitution	
<i>IXR1</i>	1	1263 C→G	Y421*	substitution	
<i>IXR1</i>	1	1075 -C	Q359K	indel	R363*
<i>IXR1</i>	1	994 C→T	Q332*	substitution	
<i>PSF3</i>	1	569 G→A	W190*	substitution	
<i>PSF3</i>	1	53 G→T	C18F	substitution	
<i>TOP1</i>	1	-243 G→A	promoter	substitution	
<i>TOP1</i>	1	1257 A→T	L419F	substitution	catalytic core
<i>DPB2</i>	1	64 T→C	Y22H	substitution	
<i>DPB2</i>	1	1064 C→T	T355I	substitution	
<i>PSF1</i>	1	599 T→A	I200N	substitution	
<i>DPB11</i>	1	1804 +A	P602*	substitution	
<i>SLD5</i>	1	388 G→A	E130K	substitution	
<i>CHL1</i>	1	2050 G→A	D684N	substitution	helicase domain
<i>RFC1</i>	1	-156 +A	promoter	indel	
<i>TOF1</i>	1	1244 C→A	P415Q	substitution	
<i>CSM3</i>	1	370 G→C	V124L	substitution	

**C****D****E****F**

65

66 **Figure S4. Related to Fig. 4. (A)** Genome-wide DNA replication profiles of wt, the *ctf4Δ* ancestor, and two  
67 double mutant strains: *ctf4Δ sld5-E130K* and *ctf4Δ ixr1Δ*.  $t_{rep}$  refers to the time at which 50% of the cells in  
68 the population replicated a region.  $t_{rep}$  was derived from the change in DNA copy numbers over time,  
69 measured by deep sequencing (see material and methods). **(B)** Mutations affecting genes implicated in  
70 DNA replication that were found in evolved clones. **(C)** Schematic representation of the two replication forks  
71 arising from an origin of replication, and the related signal they generate in the replication profiles. **(D)**  
72 Mutations affecting *Ixr1* found in evolved clones. Note that one stop codon (Q332\*) resulted from an  
73 upstream frameshift. **(E)** Fitness effect of *sld5-E130K* on *ctf4Δ* ancestor cells (left panel) and on wt, *CTF4*  
74 cells (right panel). The fitness measurements are relative to *ctf4Δ* and wt respectively. Error bars represent  
75 standard deviations. **(F)** Effect of altered levels on deoxyribonucleotide triphosphates (dNTPs) on ancestor  
76 cells. Error bars represent standard deviations. *ctf4Δ* ancestor cells carrying a conditional  $P_{GAL1}$ -*SML1* allele  
77 were used. *Sml1* is an inhibitor of the ribonucleotide reductase, an enzyme essential for dNTP production.  
78 *SML1* was expressed from the *GAL1* promoter, that is inhibited by glucose and strongly activated by  
79 galactose. A *ctf4Δ P<sub>GAL1</sub>-SML1* strain was pre-cultured in YP + 2% raffinose and then competed against a  
80 *ctf4Δ* reference strain either in YP + 2% glucose (left side), or in YP + 2% galactose 2% raffinose (right  
81 side). This should result in dNTP overproduction (glucose) and shortage (galactose).

82



83

84 **Figure S5. Related to Fig. 5. (A)** Fitness of population EVO5 relative to wt ( $s=0$ ) measured every 50  
 85 generations during the experiment (upper panel, dark plot, left y axis) with the frequency of mutant alleles  
 86 included for reference (upper panel, faint plots, right x axis). Error bars represent standard deviations.  
 87 Phylogenetic tree for clones isolated from population 5 (lower panel). Linkage was derived from analyzing  
 88 whole genome sequences of the individual clones (TableS1), while branch length was inferred from the  
 89 allele frequencies obtained by Sanger sequencing. **(B)** Frequencies of putative adaptive mutations in the  
 90 cohesion, replication and checkpoint modules in the evolved populations at the conclusion of the  
 91 experiment (generation 1000). The putative adaptive mutations were inferred based on results obtained for  
 92 population EVO5. When the experimentally validated genes were not present, closely interacting genes  
 93 were considered. Alleles frequencies in populations were obtained by deep sequencing of genomic DNA  
 94 extracted from a population sample.